Mass-Preserving Motion Correction of Dual Gated Cardiac PET

Fabian Gigengack, Lars Ruthotto, Martin Burger,
Carsten H. Wolters, Xiaoyi Jiang, *Senior Member, IEEE,* and Klaus P. Schäfers

***Abstract*—Image degradation due to motion is a known problem in positron emission tomography (PET). To reduce motion artifacts in PET, gating based techniques were found applicable. In pure respiratory gated PET, each gate still contains cardiac motion. Analogously, pure cardiac gated PET images still contain respiratory motion. Hence, we make use of dual (joint respiratory and cardiac) gating to further reduce the amount of motion contained in the images. The inclusion of non-rigid cardiac motion leads to intensity modulations caused by the partial volume effect (PVE). To overcome the intensity modulations we identified and considered the mass-preserving property of PET images in the Variational Algorithm for Mass-Preserving Image REgistration (VAMPIRE). The aim of this paper is the elimination of both cardiac and respiratory motion in thoracic dual gated PET without a loss of statistic. The strategy of our proposed motion correction approach is: 1) Dual gating, 2) Mass-preserving motion estimation (VAMPIRE), and 3) Averaging of the aligned images. In a patient study we showed that the proposed mass-preserving motion correction strategy significantly removes motion artifacts in cardiac PET. VAMPIRE achieved accurate results that resemble cardiac and respiratory motion across all patients.**

***Index Terms*—motion correction, mass-preservation, image registration, dual gating, hyperelastic regularization, PET**

I. Introduction

Image degradation due to motion is a known problem in positron emission tomography (PET) [1], [2], [3]. Gating based techniques were found applicable to reduce motion artifacts in PET. Gating is the decomposition of the whole dataset into parts that represent different breathing and/or cardiac phases [4]. After gating each single gate shows less motion.

In the context of respiratory motion correction, Dawood et al. [3] propose an optical flow based approach and Bai et al. [2] use a regularized B-spline approach with a Markov random field regularizer. However, in pure respiratory gated PET, each gate still contains cardiac motion. Analogously, pure cardiac gated PET images still contain respiratory motion. Hence, we make use of dual (joint respiratory and cardiac) gating [5] to further reduce the amount of motion contained in the images.

The inclusion of non-rigid cardiac motion leads to intensity modulations caused by the partial volume effect (PVE). To overcome the intensity modulations we identified and considered the mass-preserving property of PET images in the Variational Algorithm for Mass-Preserving Image REgistration (VAMPIRE) [1], [6], [7].

The strategy of our proposed motion correction approach is: 1) Dual gating, 2) Mass-preserving motion estimation (VAMPIRE), and 3) Averaging of the aligned images.

This work was partly funded by the Deutsche Forschungsgemeinschaft, SFB 656 MoBil (projects B2 and B3) and projects BU2327/2-1, JU445/5-1 and WO1425/1-1.

F. Gigengack is with the European Institute for Molecular Imaging (EIMI) and the Department of Mathematics and Computer Science, University of Münster, Germany.

L. Ruthotto is with the Institute of Mathematics and Image Computing (MIC), University of Lübeck, Germany.

M. Burger is with the Institute for Computational and Applied Mathematics, University of Münster, Germany.

C. H. Wolters is with the Institute for Biomagnetism and Biosignalanalysis, University of Münster, Germany.

X. Jiang is with the Department of Mathematics and Computer Science, University of Münster, Germany.

K. Schäfers is with the European Institute for Molecular Imaging (EIMI), University of Münster, Germany.

Corresponding author: fabian.gigengack@uni-muenster.de.

II. Materials and Methods

A. Dual gating of patient data in thoracic PET

An $n \times m$ dual gating [5] matrix of n cardiac and m respiratory images is built, i.e., each cardiac phase is over again divided into all respiratory phases (or vice versa). The number of gates was set to $m = n = 5$ for all computations in the following.

Information about the cardiac cycle was provided by an ECG signal. A gating scheme with equidistant time frames was performed for the cardiac cycle. This ensures similar statistics and noise levels in each gate.

The respiratory phases were estimated by a list mode data driven approach [4]. An amplitude based subdivision was performed which again ensures similar statistics per gate.

All images were reconstructed with an EM algorithm [8], [9] which is freely available at [10].

B. VAMPIRE - *Variational Algorithm for Mass-Preserving Image REgistration*

Each template image $\mathcal{T} : \Omega \to \mathbb{R}$ is registered onto an assigned reference image $\mathcal{R} : \Omega \to \mathbb{R}$, where $\Omega \subset \mathbb{R}^3$ is the image domain. This yields a transformation $y : \mathbb{R}^3 \to \mathbb{R}^3$ representing point-to-point correspondences between $\mathcal{T}$ and $\mathcal{R}$. To find y, the following functional has to be minimized

$$\min_y \ \mathcal{D}(\mathcal{M}(\mathcal{T}, y),\ \mathcal{R}) + \alpha\, \mathcal{S}(y)\ . \tag{1}$$

$\mathcal{D}$ denotes the distance functional (sum-of-squared differences (SSD) in our case) and $\mathcal{M}$ the transformation model. $\mathcal{S}$ is the regularization functional. To achieve a high robustness against noise, $\mathcal{S}$ is set to a hyperelastic regularization energy [11] which controls changes in length, area and volume of the transformation.

In the mass-preserving transformation model of VAMPIRE the template image $\mathcal{T}$ is transformed by interpolation on the deformed grid y with an additional multiplication by the volumetric change [6], [7], [12].

$$\mathcal{M}^{\text{MP}}(\mathcal{T}, y) := (\mathcal{T} \circ y) \cdot \det(\nabla y) = \mathcal{T}(y) \cdot \det(\nabla y)\ . \quad (2)$$

The implementation is based on the freely available FAIR toolbox [13] in MATLAB®. We use a multi-level strategy along with a Gauss-Newton optimization, and a spline-interpolation scheme. The VAMPIRE code can be downloaded at [14].

C. Hyperelastic regularization

The hyperelastic regularization functional $\mathcal{S}^{\text{hyper}}$ controls changes in length, area of the surface and volume of y [11]:

$$\begin{aligned}&\mathcal{S}^{\text{hyper}}(y, \alpha_l, \alpha_a, \alpha_v)\\ &\quad = \alpha_l \cdot \mathcal{S}^{\text{length}}(y) + \alpha_a \cdot \mathcal{S}^{\text{area}}(y) + \alpha_v \cdot \mathcal{S}^{\text{vol}}(y), \quad (3)\end{aligned}$$

where $\alpha_l, \alpha_a, \alpha_v > 0$ are constants and $\Gamma_a, \Gamma_v : \mathbb{R} \to \mathbb{R}$ are positive and strictly convex functions, with Γ_v satisfying $\lim_{z\to 0^+} \Gamma_v(z) = \lim_{z\to\infty} \Gamma_v(z) = \infty$. The three summands individually control changes in length, area of the surface and volume,

$$\mathcal{S}^{\text{length}}(y) := \int_\Omega \|\nabla y\|_2^2 \, dx \quad (4)$$

$$\mathcal{S}^{\text{area}}(y) := \int_\Omega \Gamma_a(\|\text{Cof}(\nabla y)\|_2^2) \, dx \quad (5)$$

$$\mathcal{S}^{\text{vol}}(y) := \int_\Omega \Gamma_v(\det(\nabla y)) \, dx\ , \quad (6)$$

where the Frobenius norm is defined as $\|A\|_2 := \sqrt{\text{tr}(A^T A)}$ for matrices $A \in \mathbb{R}^{d\times d}$ and $\text{Cof}(A)$ denotes the cofactor matrix.

D. Evaluation

As no ground-truth information for the patient data is available, the performance of our method is evaluated with image and transformation based methods. The image based method is the normalized cross correlation (NCC):

$$\text{NCC}(\mathcal{T}, \mathcal{R}) := \frac{\langle \mathcal{T}_u, \mathcal{R}_u \rangle}{\|\mathcal{T}_u\| \, \|\mathcal{R}_u\|}\ , \quad (7)$$

where $\mathcal{T}_u = \mathcal{T} - \mu(\mathcal{T})$ and $\mathcal{R}_u = \mathcal{R} - \mu(\mathcal{R})$ are the unbiased versions of $\mathcal{T}$ and $\mathcal{R}$ ($\mu(\cdot)$ is the expected value).

For validation based on the transformation, the range of the determinant of the transformation's Jacobian (Jacobian map) is analyzed. A positive and finite range indicates a diffeomorphic, i.e. invertible, transformation.

III. RESULTS

^{18}F-FDG PET data of 15 cardiac patients (20 minutes scans) were processed by dual gating and motion corrected by applying our VAMPIRE algorithm. The gate representing mid-expiration and the diastole was chosen as reference $\mathcal{R}$ as the heart is most of the time in diastole and as the mid-expiration phase shows the smallest deformation (caused by respiration) to the other gates on average.

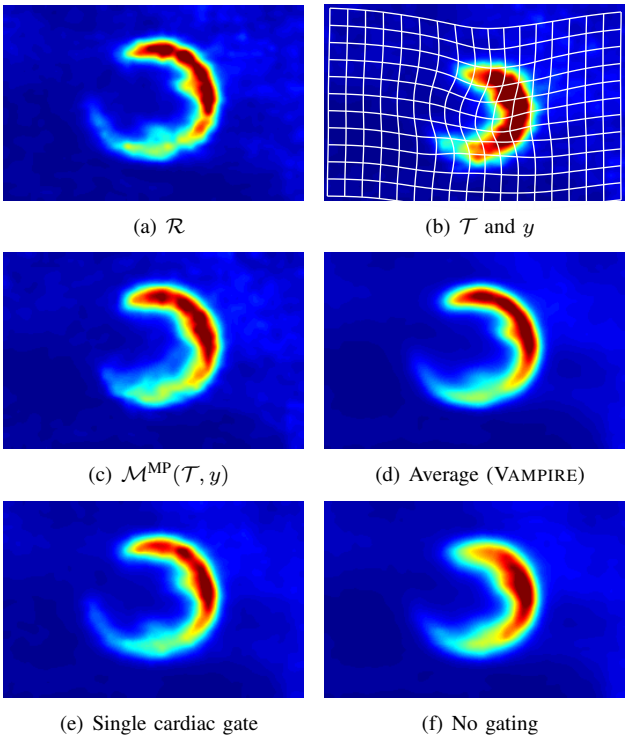

(a) $\mathcal{R}$ (b) $\mathcal{T}$ and y (c) $\mathcal{M}^{\text{MP}}(\mathcal{T}, y)$ (d) Average (VAMPIRE) (e) Single cardiac gate (f) No gating

Fig. 1. $\mathcal{T}$ (b) is registered to $\mathcal{R}$ (a) using VAMPIRE resulting in (c). Our final result after averaging all dual gates (d) and the image without any corrections (f) are shown as well. For comparison, a single cardiac gate is shown in (e).

For one patient and one gate we illustrate our results in Fig. 1 with coronal slices. The displayed template gate in (b) shows the systolic heart phase in maximum inspiration, which is the most challenging gate compared to the reference gate (a) in diastole and mid-expiration. The estimated transformation y is overlaid in (b). The mass-preserving transformed template gate can be seen in (c). The final image after averaging all aligned dual gates is shown in (d). In (f), the image without any corrections can be seen. For better comparableness with pure cardiac gating as done in [6] we show a single cardiac gate (heart in diastole) in (e).

The minimum of all Jacobian maps (all patients and all gates) is 0.340 and the maximum is 1.969. The range of the Jacobian map for each patient is further illustrated in Fig. 2. The minimum and maximum value over all gates is plotted for each patient.

On average the NCC for all patients and all gates increased from 0.902 ± 0.037 to 0.974 ± 0.001. For the most challenging gates in relation to the reference gate, i.e., heart in systole and maximum inspiration, we found an increase from 0.766 ± 0.071 to 0.969 ± 0.012. Fig. 3 illustrates the NCC values averaged over all patients.

IV. DISCUSSION AND CONCLUSION

The aim of this paper is the elimination of both cardiac and respiratory motion in thoracic dual gated PET without

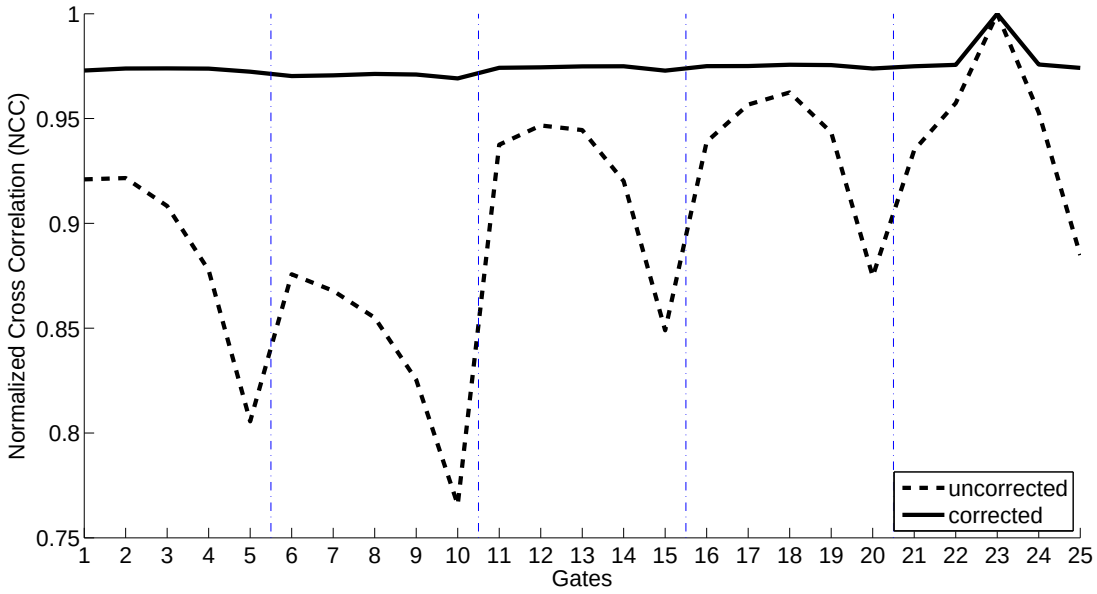

Fig. 3. The average NCC (average of all patients) before (dashed black line) and after (solid black line) motion correction is plotted for all dual gates. The blue dash-dotted lines separate the different cardiac gates which consist of five respiratory gates each. The reference image is gate 23 which explains the NCC value of one.

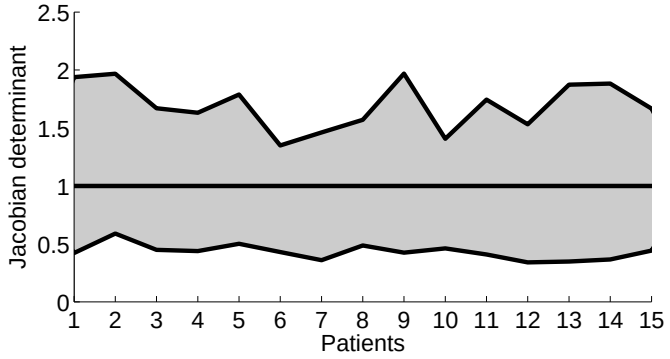

Fig. 2. The global minimum and maximum of the Jacobian map is shown for each of the 15 patients. The gray area represents the range of the Jacobian maps. Values below 1 represent expansion and values above 1 compression. Hence, all transformations are diffeomorphic as no values below 0 appear.

a loss of statistic. In a study of 15 patients we showed that the proposed mass-preserving motion correction strategy significantly removes motion artifacts in cardiac PET. The results of VAMPIRE are accurate and resemble cardiac and respiratory motion across all patients. This is indicated by good NCC values and appropriate Jacobian ranges (i.e. no negative or too large values appear) that guarantee invertibility of the estimated transformations.

The dual gating scheme leads to a lower statistic per gate due to the increased number of gates compared to pure respiratory or pure cardiac gating. This demands adequate regularization. Hyperelastic regularization makes VAMPIRE robust against noise as length, area and volume of the transformation can be controlled.

The average image in Fig. 1(d) combines the reduced amount of motion of the reference gate (a) with the low noise of the image without gating (f). The superiority of dual gating compared with pure cardiac gating [6] can be seen, e.g., at the upper part of the heart contour in Fig. 1(d) and (e).

We are positive that further improvements of image quality can be achieved by a joint reconstruction of image and motion or by incorporating the transformation into a motion compensated reconstruction, which is left for future work.

In conclusion, we propose a novel image registration approach to motion correction in thoracic PET. The major improvement is the incorporation of a mass-preserving transformation model in combination with dual gating for motion estimation. We show that both cardiac and respiratory motion are robustly eliminated to a very high extent.

V. ACKNOWLEDGMENTS

The authors would like to thank Thomas Kösters for providing his reconstruction software EMRECON used for reconstruction. The list mode-driven gating was performed with the help of Florian Büther and his gating software. Especially, we thank Jan Modersitzki for his advise regarding the implementation and for making his FAIR toolbox freely available.

REFERENCES

[1] F. Gigengack, L. Ruthotto, M. Burger, C. Wolters, X. Jiang, and K. Schäfers, "Motion correction in dual gated cardiac pet using mass-preserving image registration," *IEEE Trans. Med. Imag.*, In press.

[2] W. Bai and M. Brady, "Motion correction and attenuation correction for respiratory gated PET images," *IEEE TMI*, vol. 30, no. 2, pp. 351–365, 2011.

[3] M. Dawood, F. Büther, X. Jiang, and K. Schäfers, "Respiratory motion correction in 3-D PET data with advanced optical flow algorithms," *IEEE TMI*, vol. 27, no. 8, pp. 1164–1175, 2008.

[4] F. B. et al., "List mode-driven cardiac and respiratory gating in PET," *J. Nucl. Med.*, vol. 50, no. 5, pp. 674–681, 2009.

[5] A. Martinez-Möller, D. Zikic, R. Botnar, R. Bundschuh, and W. H. et al., "Dual cardiac–respiratory gated PET: Implementation and results from a feasibility study," *EJNMMI*, vol. 34, pp. 1447–1454, 2007.
[6] F. Gigengack, L. Ruthotto, M. Burger, C. Wolters, X. Jiang, and K. Schaefers, "Motion correction of cardiac PET using mass-preserving registration," in *NSS/MIC Conference Record, IEEE*, 2010.
[7] L. Ruthotto, "Mass-preserving registration of medical images," German Diploma Thesis (Mathematics), Institute for Computational and Applied Mathematics, University of Münster, march 2010.
[8] T. Kösters, K. Schäfers, and F. Wübbeling, "EMRECON: An expectation maximization based image reconstruction framework for emission tomography data," in *NSS/MIC Conference Record, IEEE*, 2011.
[9] T. Kösters, "Derivation and analysis of scatter correction algorithms for quantitative positron emission tomography," Ph.D. dissertation, University of Münster, 2010.
[10] [Online]. Available: http://emrecon.uni-muenster.de
[11] M. Droske and M. Rumpf, "A variational approach to nonrigid morphological image registration," *SIAM J. Appl. Math.*, vol. 64, no. 2, pp. 668–687, 2003.
[12] K. Thielemans, E. Asma, and R. Manjeshwar, "Mass-preserving image registration using free-form deformation fields," in *NSS/MIC Conference Record, IEEE*, 2009.
[13] J. Modersitzki, *FAIR: Flexible Algorithms for Image Registration*. Philadelphia: SIAM, 2009.
[14] [Online]. Available: http://vampire.uni-muenster.de